Supplementary Material for "Salt dependence of the radius of gyration and flexibility of single-stranded DNA in solution probed by small-angle x-ray scattering"

Adelene Y.L. Sim[1], Jan Lipfert[2], Daniel Herschlag[3], Sebastian Doniach[1,4,5]

[1]*Applied Physics Department, Stanford University*

[2]*Department of Bionanoscience, Kavli Institute of Nanoscience, Delft Institute of Technology, The Netherlands*

[3]*Biochemistry Department, Stanford University, Stanford, California 94305, USA*

[4]*Physics Department, Stanford University, Stanford, California 94305, USA*

[5]*Biophyics Program, Stanford University, Stanford, California 94305, USA*

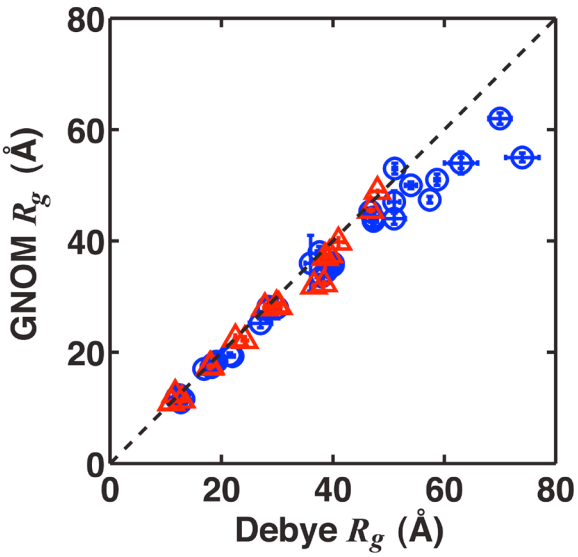

Figure S1: Radius of gyration (R_g) obtained by fitting to the Debye function (see main text) to small-angle x-ray scattering data are comparable to R_g obtained by regularized inversion of data using the program GNOM [1]. This latter approach requires the determination of the maximum pair-wise distance, D_{max}, which was estimated visually as the lowest value required for a smooth fit to the data, as values of D_{max} beyond the initial best fit often lead to overfitting of the data, and hence erroneous estimates of the maximum pair-wise distance. Variations of D_{max} (± 5 Å) and repeat measurements were used to estimate to the error in R_g. R_g for poly-T and poly-A are illustrated as blue circles and red triangles respectively. Most R_g values are equivalent (black dashed line), but more significant deviations are observed for the largest R_g values: the R_g values from GNOM above 60 Å (for poly-T65 and poly-T100) are consistently lower than those from Debye fitting.

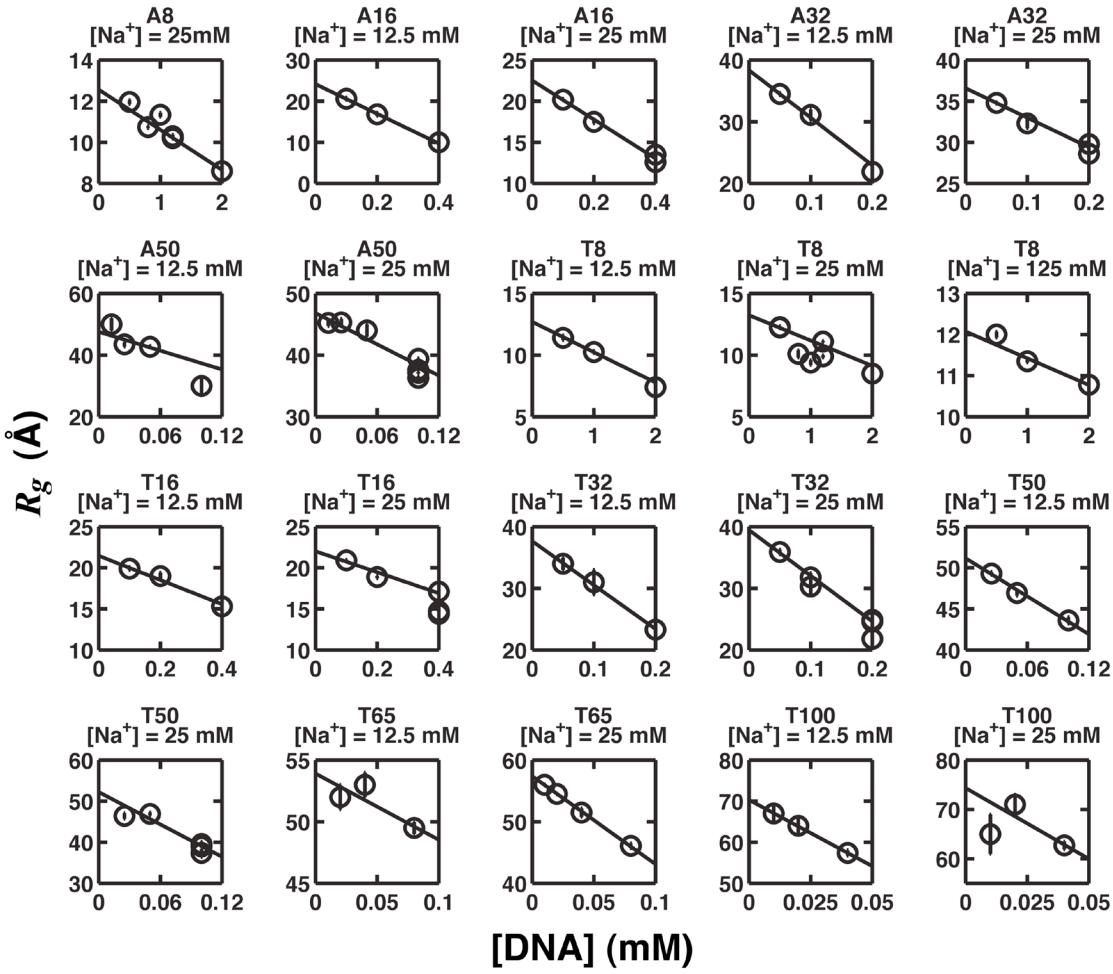

Figure S2: Extrapolation of the measured radii of gyration to zero DNA concentration. Multiple measurements for each DNA length at each ionic condition were made to probe for inter-particle interference. If the scattering profiles do not superimpose and therefore show dependence on DNA concentration ([DNA]), radii of gyration (R_g) were individually fitted then plotted as a function of [DNA]. The lack of superimposability between profiles for different [DNA] was mostly observed only for low salt conditions, likely a consequence of inter-particle interference arising from electrostatic repulsion. The linear fit between R_g and [DNA] was determined (black lines) and extrapolated to zero [DNA] to obtain the R_g value in the absence of inter-particle interference. (See the figure titles for the corresponding experimental conditions.)

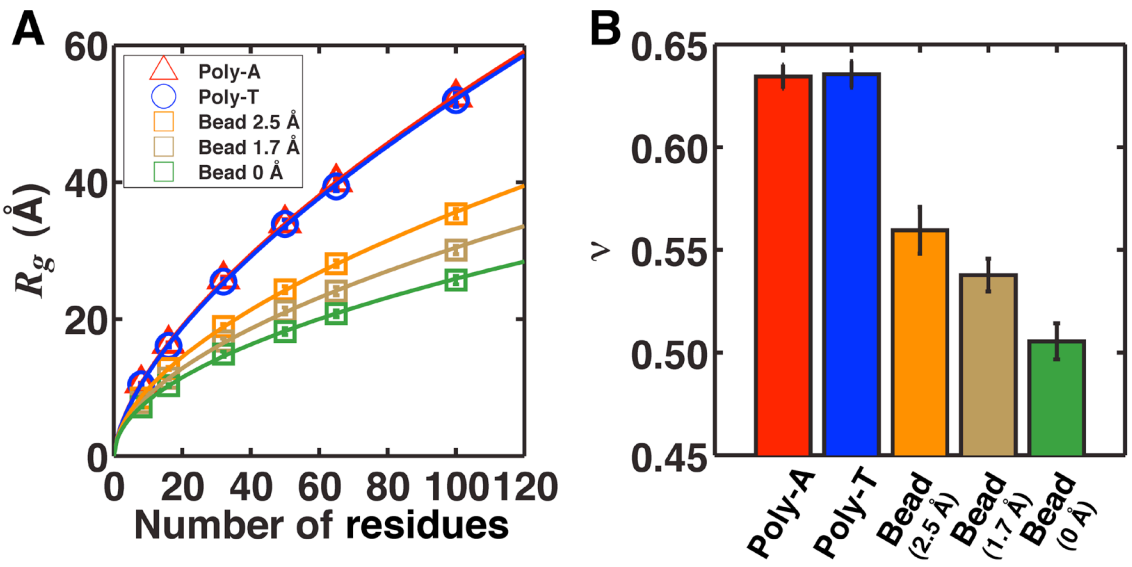

Figure S3: The scaling of the radius of gyration with chain length as determined by different simulations. Five different simulation results are shown: "sterics only" simulations of poly-A and poly-T (red triangles and blue circles respectively); "beads on a string" model with bead radii of 2.5, 1.7 and 0 Å (orange, brown and green squares or bars respectively) and distance between beads of 6.5 Å (identified as the effective monomer length from the persistence length fits; see main text). (**A**) The simulated radii of gyration (R_g) as a function of the number of bases. The fitted scaling curves are shown as lines. (**B**) The corresponding fitted scaling exponents (ν).

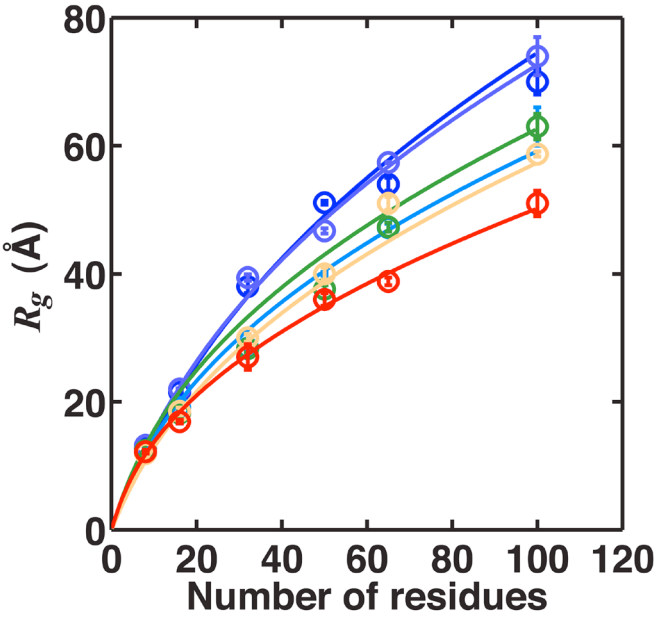

Figure S4: Determining poly-T persistence length by fitting radius of gyration to the worm-like chain model. Results are color-coded for different concentrations of Na^+: 12.5 mM (dark blue), 25 mM (light blue), 125 mM (cyan), 225 mM (green), 525 mM (yellow), 1025 mM (red). The persistence lengths and effective monomer lengths from these fits are summarized in Table S3.

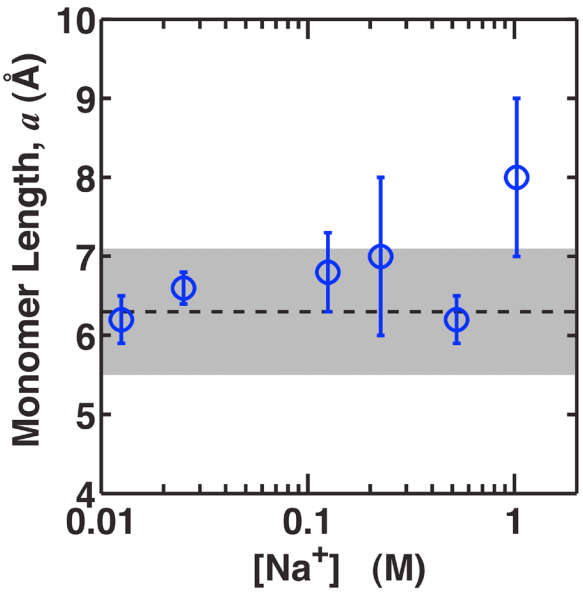

Figure S5: The monomer length (a) obtained by persistence length fitting of the poly-T data using the R_g scaling law (see main text) shows small salt dependence and is consistent with the value determined by crystal structure analysis [2] (6.3 ± 0.8 Å; dashed black line, standard deviation indicated by shaded gray). The full dataset fits to a gradual linear increase in a at a rate of 0.55 log([Na^+]). However, if we neglect the data point at 500 mM, a increases linearly at a rate 0.84 log([Na^+]), whereas excluding a at 1 M Na^+ yields a much weaker dependence of 0.12 log([Na^+]).

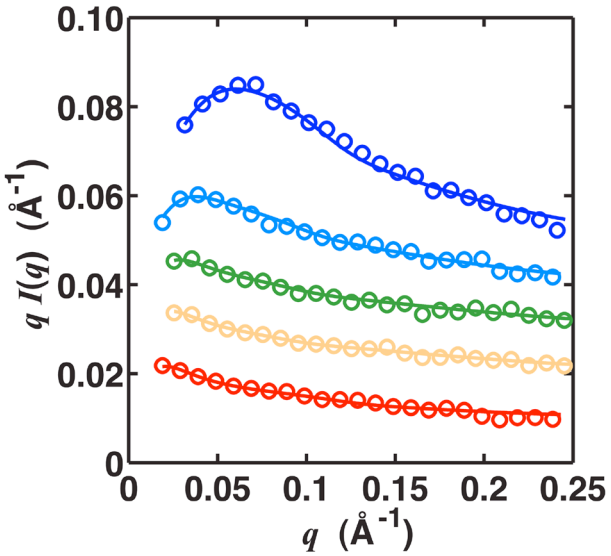

Figure S6: Examples of fitting full scattering profiles to the worm-like chain model to determine persistence lengths of poly-T under different salt conditions. The experimental data points are shown as circles (only one in every 20 points is shown for clarity) and the fitted worm-like chain functions are shown as lines. The 8-mer was excluded from this fitting since its contour length is smaller than four-times the persistence length and therefore requires a different functional form for the fit [3]. Illustrated here are the fits to T16 (blue), T32 (cyan), T50 (green), T65 (yellow) and T100 (red) respectively at [Na^+] = 25 mM. The monomer contour length a was set at 6.5 Å for these fits. Without fixing a, fits often did not converge or resulted in an unphysical a that varied significantly for the same salt condition but different N. Profiles are vertically offset for clarity.

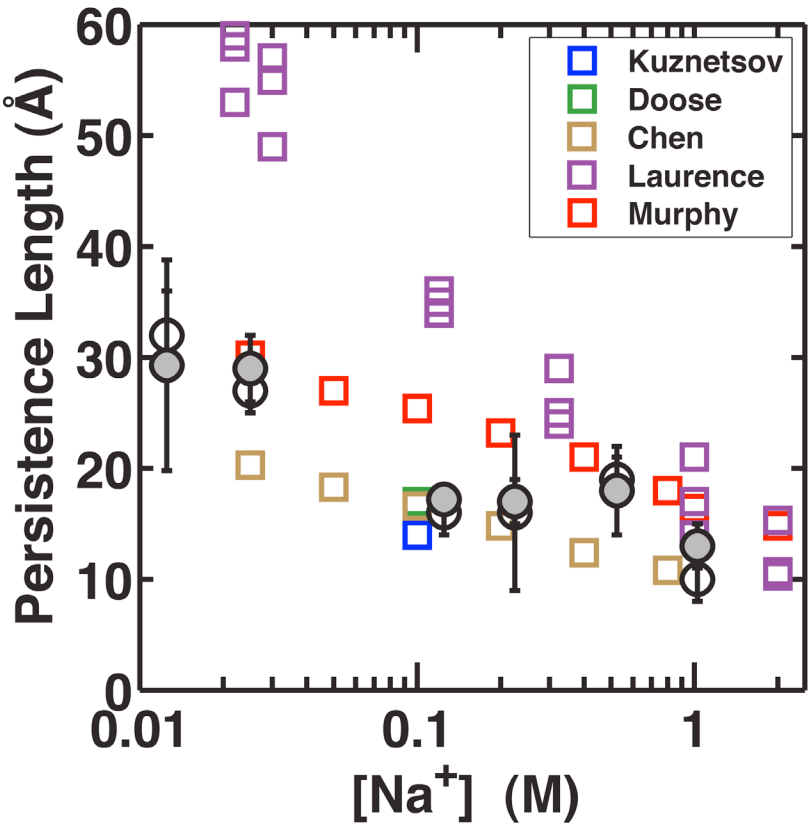

Figure S7: Comparison of persistence lengths determined using different experimental methods ([2, 4-7]; see legend and Table S4) and those obtained in our study (worm-like chain fitting to R_g scaling in black circles and fitting individual scattering profiles in gray filled circles respectively). Results summarized in Table S4 that measures persistence lengths of other sequences (not poly-T) and in other ionic conditions are omitted.

[Na^+] (mM)	R_g (Å)									
	Poly-A				Poly-T					
	A8	A16	A32	A50	T8	T16	T32	T50	T65	T100
12.5	N.D.	24.2 ± 0.5	38.4 ± 0.7	48 ± 1	12.7 ± 0.3	21.5 ± 0.3	38 ± 1	51.1 ± 0.3	54 ± 1	70 ± 2
25	12.90 ± 0.08	22.5 ± 0.2	26.6 ± 0.8	46.8 ± 0.5	13.2 ± 0.09	22.0 ± 0.1	39.4 ± 0.5	46.7 ± 0.4	57.4 ± 0.1	74 ± 3
125	N.D.	N.D.	N.D.	N.D.	12.07 ± 0.05	19.1 ± 0.2	28.4 ± 0.6	40.0 ± 0.3	47.2 ± 0.6	63 ± 3
225	11.0 ± 0.3	18.0 ± 0.3	29.9 ± 0.8	41 ± 1	12.42 ± 0.05	18.2 ± 0.8	28.3 ± 0.6	37.6 ± 0.6	47.3 ± 0.7	63 ± 2
525	11.7 ± 0.1	18.1 ± 0.5	30.3 ± 0.4	39.4 ± 0.3	11.9 ± 0.4	18.5 ± 0.6	30.0 ± 0.6	40 ± 1	51 ± 1	58.7 ± 0.4
1025	11.0 ± 0.3	17.9 ± 0.1	27.8 ± 0.2	38.6 ± 0.4	12.2 ± 0.3	16.9 ± 0.3	27 ± 2	36 ± 1	38.8 ± 0.6	51 ± 2

Table S1: Summary of radii of gyration (R_g) obtained by fitting to the Debye function (see main text) for poly-A and poly-T at different salt conditions. N.D.: Not determined.

[Na^+] (mM)	Poly-A	Poly-T
12.5	N.D.	0.724 ± 0.009
25	0.730 ± 0.005	0.691 ± 0.003
125	N.D.	0.652 ± 0.004
225	0.72 ± 0.02	0.625 ± 0.005
525	0.665 ± 0.007	0.61 ± 0.01
1025	0.664 ± 0.009	0.58 ± 0.01

Table S2: Summary of scaling exponent (ν) for poly-A and poly-T obtained at different salt conditions by fitting radii of gyration (R_g) to the scaling form $R_g \propto N^{\nu}$ where N is the number of monomers. Scaling fit for poly-A at 12.5 mM was omitted due to the absence of A8 measurement at this ionic condition. N.D.: Not determined.

[Na^+] (mM)	Scaling fit		Scattering profile fit
	a (Å)	L_p (Å)	L_p (Å)
12.5	6.2 ± 0.3	32 ± 4	29.3 ± 9.5
25	6.6 ± 0.2	27 ± 2	29 ± 3
125	6.8 ± 0.5	16 ± 2	17.2 ± 0.5
225	7 ± 1	16 ± 7	17 ± 2
525	6.2 ± 0.3	19 ± 2	18 ± 4
1025	8 ± 1	10 ± 2	13 ± 2

Table S3: Summary of persistence length (L_p) and effective monomer length (a; scaling fit only) for poly-T obtained by two different fitting schemes under different salt conditions.

Solution condition	L_p (Å)	Experimental Method	Sequence	Ref.
Denaturing	31 ± 3 ≤ L_p ≤ 52 ± 5	Fluorescence recovery after photobleaching after thermal denaturation	Mixed sequence	[8]
100 mM NaCl	14	Optical melting	Poly-T	[4]
100 mM NaCl	17	Fluorescence correlation spectroscopy	Poly-T100	[5]
150 mM NaCl	7.5	Single molecule optical strap	Mixed sequence	[9]
0 – 800 mM NaCl	11 – 22	Small angle x-ray scattering and single molecule Förster resonance energy transfer	Poly-T40	[6]
20 mM – 2 M NaCl	10 – 60	Single molecule Förster resonance energy transfer	Poly-T	[7]
25 mM – 2 M NaCl	15 – 30	Fluorescence spectroscopy	Poly-T	[2]
10 mM NaCl and 2 mM $MgCl_2$	13	Scanning force microscopy	Up to 5 single stranded bases	[10]
3-8 mM Mg^{2+}	31	Transient electric birefringence	Poly-T	[11]
3-8 mM Mg^{2+}	78 ± 8	Transient electric birefringence	Poly-A	[11]
0 – 100 mM $MgCl_2$	8 – 22	Small angle x-ray scattering and single molecule Förster resonance energy transfer	Poly-T40	[6]

Table S4: Summary of the persistence lengths (L_p) measured at different solution conditions using different experimental methods and sequences.

References

[1] D. I. Svergun, J Appl Crystallogr 25, 495 (1992).
[2] M. C. Murphy *et al.*, Biophys J 86, 2530 (2004).
[3] J. S. Pedersen, and P. Schurtenberger, Macromolecules 29, 7602 (1996).
[4] S. V. Kuznetsov *et al.*, Biophys J 81, 2864 (2001).
[5] S. Doose, H. Barsch, and M. Sauer, Biophys J 93, 1224 (2007).
[6] H. Chen *et al.*, Proc Natl Acad Sci USA 109, 799 (2012).
[7] T. A. Laurence *et al.*, Proc Natl Acad Sci USA 102, 17348 (2005).
[8] B. Tinland *et al.*, Macromolecules 30, 5763 (1997).
[9] S. B. Smith, Y. Cui, and C. Bustamante, Science 271, 795 (1996).
[10] C. Rivetti, C. Walker, and C. Bustamante, J Mol Biol 280, 41 (1998).
[11] J. B. Mills, E. Vacano, and P. J. Hagerman, J Mol Biol 285, 245 (1999).